ELSEVIER

Journal of Electroanalytical Chemistry 528 (2002) 1–17

Journal of Electroanalytical Chemistry

www.elsevier.com/locate/jelechem

Some problems on the resistance method in the in situ measurement of hydrogen content in palladium electrode

Wu-Shou Zhang *, Zhao-Fu Zhang, Zhong-Liang Zhang

Institute of Chemistry and Center for Molecular Science, Chinese Academy of Sciences, P.O. Box 2709, Beijing 100080, People's Republic of China

Received 21 January 2002; received in revised form 25 March 2002; accepted 3 April 2002

Abstract

Some problems on the resistance method in determining the hydrogen content in PdH_x electrodes are discussed. First, the resistivity ratio of PdH_x, the temperature coefficient of resistivity and the resistance of PdH_x, and the resistance of Pd having undergone hydriding–dehydriding cycles are discussed. It is found that the resistivity ratio is somewhat higher than the resistance ratio with the same x value and their difference depends on the internal stress-state arising from hydrogen insertion. Another fact that has been omitted in past work is that the temperature coefficients of PdH_x resistance and resistivity increase while $x > 0.7$. The Pd resistance decreases with hydriding–dehydriding cycle number due to the shape deformation of the electrode, which occurs. Second, the effect of the non-uniform distribution of x in the electrode on determining the hydrogen content is discussed theoretically. It is proved that errors are particularly significant when the Pd+H system is in the mixed $\alpha+\beta$ phase or the resistance is near the maximum value. Finally, we calculate the additional potential drop and hence the apparent resistance of the PdH_x electrode caused by the co-conduction of electrolyte, the concentration-cell effect, the collection of electrolysis current and other imperfect configurations of the electrode in the in situ measurement of electrode resistance, using a direct current. It is found that an electrode with a large ratio of length to radius, an active surface, a surrounding electrolyte with high conductance and a high electrolysis current will all induce substantial additional resistance. At the same time, some advice on measuring the PdH_x resistance is presented. © 2002 Published by Elsevier Science B.V.

Keywords: Pd electrode; Resistance; Concentration-cell; Hydrogen evolution; Diffusion

1. Introduction

It has long been recognized that the electrical resistance of palladium loaded with hydrogen (taken to include deuterium, as below) is a function of the hydrogen content [1–45]. This relationship is always expressed in terms of the resistance ratio of the palladium hydride at a particular loading (denoted by the atom ratio, $x = \mathrm{H/Pd}$) to the initial value of the free hydrogen, i.e.:

$$\chi_R = \frac{R_{\mathrm{PdH}_x}}{R_{\mathrm{Pd}}} \tag{1}$$

as shown in Fig. 1. The relationships between χ_R and x have almost the same shape for both Pd+H and Pd+D systems but, at the same x value, the resistance is somewhat larger for the Pd+D system, in particular in the high x region.

The behavior of χ_R with changing x can be summarized as follows. When a palladium sample begins to absorb hydrogen, the solid solution phase, α is formed first and the relative resistance increases almost linearly with increasing x up to the α phase boundary composition, x_α [9–11,21–23]. Then the Pd+H system is in the mixed $\alpha+\beta$ phase, χ_R increases less sharply with x up to the β phase boundary composition, x_β at which the phase transition ends [1–3,16]. With further increase of x, the Pd+H system is in the pure β phase, the increase rate of χ_R gradually decreases and reaches the maximum $\chi_{R,\max}$ at $x_{\max}$ [1–4,24,30]. In the higher x region, χ_R

Abbreviations: dc, direct current; ec, electrolysis current; ecd, electrolysis current density; emf, electromotive force; her, hydrogen evolution reaction; ISRM, in situ resistance measurement; STM, scanning transmission microscope.

* Corresponding author. Fax: +86-10-62559373

E-mail address: wszhang@infoc3.icas.ac.cn (W.-S. Zhang).

0022-0728/02/$ - see front matter © 2002 Published by Elsevier Science B.V.
PII: S0022-0728(02)00845-8

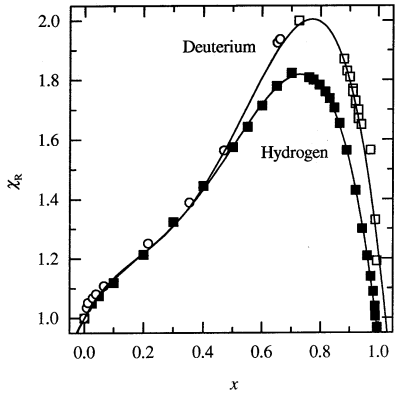

Fig. 1. Resistance vs. loading ratio for the Pd+H [30] and Pd+D [11,31] systems in the overall H (D) concentration range at 25 °C. The solid squares are data from Baranowski et al. [30], the open circles are data from Flanagan and Lewis [10] and the open squares are data from Baranowski and Filipek [31]. The contribution to the resistance induced by the high pressure in the original resistance data is extracted in this figure, and the isotherm of Wicke and Nernst [46] is used to obtain x instead of the logarithm relation between x and hydrogen pressure in the original paper [28] which can result in $x > 1$.

decreases sharply up to the saturation absorption at which stoichiometric palladium hydride, PdH is formed as was confirmed in high-pressure or low-temperature experiments [4,27–40].

A polynomial can be used to fit χ_R as a function of x in the overall hydrogen concentration region ($0 \le x \le 1$), based on the experimental data in Refs. [11,30,31,46] (see Fig. 1) and we obtain:

$$\chi_R = \begin{cases} 1 + 1.69731x - 5.34162x^2 + 13.4472x^3 - 9.87644x^4 & \text{for H} \\ 1 + 1.88402x - 6.94933x^2 + 17.2941x^3 - 12.0073x^4 & \text{for D} \end{cases} \quad (2)$$

with correlation coefficient $R^2 = 0.999$ and standard deviation $\sigma^2 = 0.01086$ for H, and $R^2 = 0.9909$ and $\sigma^2 = 0.0318$ for D. Of course, this empirical approximation may differ from some experimental results [24,53] especially for x near x_{max} due to the peaks in Fig. 1 becoming broad and gently rounded.

The behavior of χ_R with changing x can be explained by the scattering theory in solid-state physics. When hydrogen atoms are inserted into the pure palladium lattices, the disorder increases and the number of scattering centres for conduction electrons increases as well; this makes the resistance increase linearly with x. On the other hand, the pure palladium has 0.36 holes in the d band and the s–d scattering contributes substantially to the resistance [32]. This d band needs 0.55–0.60 hydrogen to fill it, so the resistance dependence for the mixed $\alpha+\beta$ phase is of course due to the combined effect of the opening up of the d band and the appearance of the α and β mixture [34,35]. At high x values ($x > 0.6$), the PdH_x looks more like an s type metal than a transition metal, which has, in general, higher resistivity than an s type metal, so it is easy to understand the low resistivity of PdH_x. When x approaches 1, the scattering centers for conduction electrons are the vacancies in the hydrogen sublattices whose number is proportional to $(1-x)$ [34], so the resistance decreases with increasing x.

The actual experimental data are scattered around those shown in Fig. 1 due to the facts below: (1) The pretreatment of the sample influences the amplitude of χ_R. Flanagan and Lewis have found that annealing the palladium at 900 °C for 1 h results in a low χ_R value whereas the quenched sample results in a high χ_R value [9]. (2) Brüning and Sieverts [6] and Lewis et al. [16] have found hysteresis of the resistance ratio during the hydriding–dehydriding process; this behavior can be understood by the differences of x_α and x_β between the absorption and desorption processes using the method which will be discussed in Section 3.4.2. (3) The dimensional changes of the electrode in the hydrogen absorption and/or desorption processes affect the resistance ratio and these changes depend on the hydriding and/or dehydriding processes, but this was not given sufficient attention in the past. The latter situation forms one of the aims of this paper.

The relationship between resistance and x has been used to infer the loading ratio in the electrolysis experiments [47–57]. In comparison with ex situ methods, e.g. gravimetric determination [9], thermal analysis [58] and coulometry [59], the resistance measurement can monitor in situ the hydrogen content which depends strongly on the electrochemical parameters, and hydrogen escapes from the electrode when it is removed from the electrolysis system. Of course, there have been other in situ methods, e.g. the volumetric method in a closed system [60], X-ray diffraction [61] and neutron reflectometry [62] used in experiments, but they have inherent defects compared with the resistance measurement. The first technique is sensitive to impurity gases and may overestimate the hydrogen concentration, and the latter two methods reveal only the local but not the overall properties, especially for a thin film sample as verified in similar experiments [63]. The advantage of the resistance method is that the resistance reflects the overall bulk properties of the sample affected by the hydrogen absorption, so it does not depend on the local characteristics and surface impurities. At the same time it has a small temperature dependence that can be calibrated using the available experimental results as will be discussed subsequently.

However, unlike the gravimetric, volumetric and coulometric techniques, the in situ resistance measurement (ISRM) does not give a direct measure of loading and hence requires calibration against one of these former techniques. This makes the reliability depend not only on the measurement of the resistance but also on the accuracy of the relationship between χ_R and x. On the other hand, the accepted resistance data are

measured in the equilibrium or quasi-equilibrium state; the practical hydrogen distribution is non-uniform most of time in ISRM in the electrolysis experiments; this non-uniformity makes the measured hydrogen concentration differ from the average value. At the same time, the electrolyte solution surrounding the electrode affects the ISRM in many ways besides the co-conduction of the measuring current through the electrolyte. The most important effects are the additional potential shifts caused by the measuring current and the electrolysis current (ec). In this paper, we will discuss these problems in turn.

2. Experimental

The electrolysis cell consisted of a glass vessel (inner ϕ 12×40 mm) and electrodes in a LiOH aqueous solution (~ 2 ml). The cathode was made of a palladium wire (ϕ 0.2×50–90 mm, 99.9% purity) wound round a PTFE rod; each cathode end was spot-welded to two platinum leads (ϕ 0.2×50 mm) for measuring H/Pd by ISRM. The anode was made of a platinum wire (ϕ 0.02×100 mm) wound round another PTFE rod. All platinum wire leads were covered with thin-walled PTFE tubes to minimize their contact with the electrolyte and catalysis of the H_2+O_2 combination. A diaphragm was used in the cell to separate the cathode and anode compartments and prevents H_2 and O_2 combination. LiOH (1 M) aqueous solution was prepared by dissolving LiOH (No. 3 reagent plant of Shanghai, AR) in deionized H_2O. The resistance was measured potentiometrically with the standard four-probe technique. The measuring currents used were 1–100 mA; the potential drops were measured by a Keithley 15OB microvolt ammeter.

3. Results and discussion

In this section, we will discuss some of the problems which occurred in the ISRM. These issues can be classified into two groups, one group including Sections 3.1, 3.2 and 3.3 is for the equilibrium state of the Pd+H system; another one including Sections 3.4, 3.5, 3.6 and 3.7 is for the non-equilibrium state which usually occurs in the ISRM. In this work, the direct current (dc) situation is focused on the ISRM, but most of the conclusions can be extended to that of alternating current except the concentration-cell effect studied in Sections 3.5.2, 3.6.2 and 3.7. Although our aim is to investigate the Pd/H electrode, the conclusions obtained in Sections 3.1, 3.2, 3.3 and 3.4 can be extended to the Pd/H_2 system and all of the results can be applied to the Pd/D electrode or the Pd/D_2 system with some parameters modified.

3.1. Resistivity ratio

From the viewpoint of physics, a resistivity ratio should be more fundamental to characterize the change of hydrogen concentration than the resistance ratio χ_R although the latter is always used in experiments. Similar to the concept of χ_R in Eq. (1), we define the resistivity ratio:

$$\chi_\rho = \frac{\rho_{PdH_x}}{\rho_{Pd}} \tag{3}$$

with ρ_{PdH_x} and ρ_{Pd} being the resistivities of PdH_x and Pd, respectively. χ_ρ is also a function of x and has a similar shape to that of χ_R shown in Fig. 1. The difference arises from the expansion effect in the hydrogen insertion into the palladium lattice. It was supposed that a sample expansion is uniform in all three dimensions in past work [32,34,41], but this is not the case in practice. The actual dilation of a PdH_x sample has two extreme situations according to whether the internal stresses arising from an inhomogeneous distribution of hydrogen (including phase transitions) in the absorption and/or desorption processes are removed or not, i.e. the coherence and incoherence expansions[1]. For the coherence situation, the lattices distort but do not crack so the expansion is uniform in all directions. In contrast, the internal stresses are released by plastic deformation in the small size direction (radius for a rod and thickness for a plate) but the large size direction (length for a rod, radius for a circular plate, and width and length for a rectangular plate) changes very little in the incoherence situation. For a general case, the expansions are between these two states. Consider a sample with uniform cross-section S and length $l \gg S^{1/2}$; the resistances in these three situations are:

$$R_{PdH_x} = \frac{\rho_{PdH_x} l_{Pd}}{S_{Pd}} \times \begin{cases} \dfrac{1 + \varepsilon_V x/3}{1 + 2\varepsilon_V x/3}, & \text{coherence} \\ \dfrac{1 + \varepsilon_l x}{1 + (\varepsilon_V - \varepsilon_l)x}, & \text{general} \\ \dfrac{1}{1 + \varepsilon_V x}, & \text{incoherence} \end{cases} \tag{4}$$

with

$$\varepsilon_V = \frac{1}{V}\frac{\partial V}{\partial x} \tag{5}$$

where ε_V is the partial volume of H in Pd expressed as the volume fraction; its average value in the overall hydrogen concentration region is 0.162 and 0.157 for H and D, respectively [64,65]. ε_l is the partial length

[1] It should be distinguished that the meanings of 'coherence' and 'incoherence' here differ from the same phrases in other disciplines, e.g. laser or solid state physics.

change. Combining Eqs. (1), (3) and (4) gives:

$$\chi_\rho = \chi_R(1+\varepsilon_R x) \tag{6}$$

with the correction factor:

$$\varepsilon_R = \begin{cases} \varepsilon_V/3, & \text{coherence} \\ \varepsilon_V - 2\varepsilon_l, & \text{general} \\ \varepsilon_V, & \text{incoherence} \end{cases} \tag{7}$$

$\varepsilon_R x$ versus x is shown in Fig. 2. It is seen that the acquisition of the resistivity ratio from the resistance ratio depends on the internal stress-state of hydrogen in palladium, hence the correction factor changes from 5.4 to 16.2% for PdH. This result also indicates that the resistance ratios obtained under different conditions may differ from each other by as much as $2\varepsilon_V x/3$, which is 10.8% for PdH. The general situation is a mixture of these two cases so we have $\varepsilon_V/3 \le \varepsilon_R \le \varepsilon_V$ and the value of ε_R depends on the preparation process of the PdH_x sample. In the hydrogen absorption and/or desorption processes at room temperature, the $\alpha \leftrightarrow \beta$ phase transition results in plastic deformation and creation of dislocations [66,67], so the incoherence situation is unavoidable in the main region of hydrogen concentration. On the other hand, the mixed $\alpha+\beta$ phase is overcome while the applied hydrogen pressure is slowly stepped up by small increments at high temperatures in some experiments [56]; it is then in the coherence situation.

In experiments, the correction factor ε_R can be obtained by the measurements of resistance, dimensions and hydrogen content of PdH_x in conjunction. It is a pity that this result has not been obtained up to now although the dimensional changes in the hydrogen absorption and/or desorption processes were monitored in early work such as that in Refs. [3,5,68,69] and other work cited in Ref. [70], so we have to use the dimensional change alone to obtain ε_R. Graham has observed that the length of a Pd wire was elongated by 1.605% by an accompanying hydrogen absorption change to $x =$ 0.677 [68], this result corresponds to $\varepsilon_l = 2.37\%$; and the data in work by Fischer [5] gives $\varepsilon_l = 3.32\%$. These two results give $\varepsilon_R = 10.5\%$ and this situation is also shown in Fig. 2 as the 'usual case'.

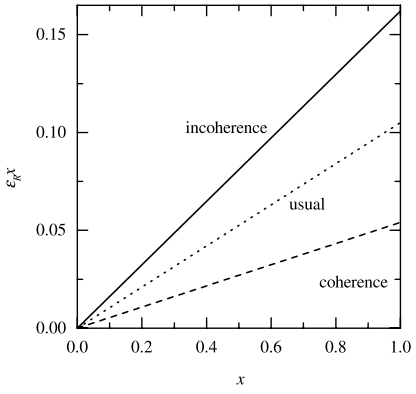

Fig. 2. Correction factor in acquiring the resistivity ratio from the resistance ratio. The dotted, solid and dashed lines are for the coherence, incoherence and usual cases of internal stress of H in Pd, respectively (detailed explanation can be found in Section 3.1).

3.2. Effect of temperature on the PdH_x resistance

Besides the experimental results on χ_R versus x around room temperature (T_R) such as those shown in Fig. 1, there is also similar work at other temperatures [6–8,10,14–17,19–21,24–26,32–43]. However, most of results are concentrated on very low temperatures due to the phenomenon of superconductivity of PdH_x (and PdD_x) with $x \ge 0.8$ at $T < 12$ K found in 1972 [71–74] and the anomaly of resistance and specific heat around 50 K with x around 0.6 found in 1957 [41,75–78]. Although some data on the temperature effect around T_R are available [10,17], a systematic study on the overall hydrogen concentration has not been carried out to date. Therefore we have to deduce the temperature coefficient from different results obtained by different authors [10,17,30,34] as is shown in Fig. 3.

In Fig. 3(a), the temperature coefficient of resistivity $\rho'_{PdH_x,T}$ around T_R with $x \le 0.685$ is obtained using the

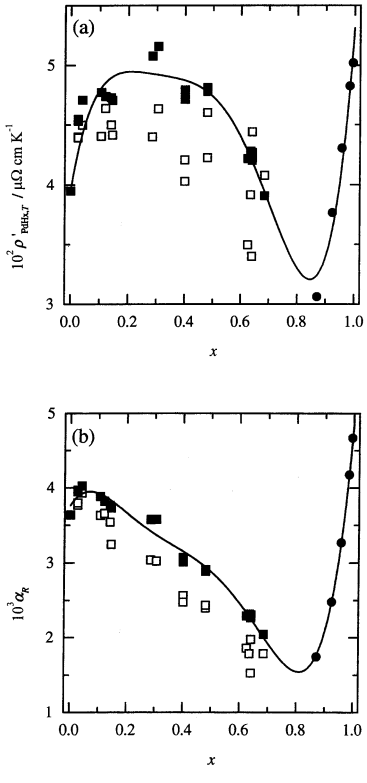

Fig. 3. The temperature coefficient of resistivity (a) and resistance (b) of PdH_x around room temperature. The open squares are data of Flanagan and Lewis [10]; the solid squares are data calculated from those of Flanagan and Lewis [10] at 0 °C and McNicholl and Lewis [17] at 65 °C; the solid circles are data obtained from Baranowski et al. [30] at 25 °C and Burger et al. [34] at −77 °C. All the data in (a) have been corrected for the expansion effect.

data of Flanagan and Lewis [10] at 0 °C and McNicholl and Lewis [17] at 65 °C; $\rho'_{PdH_x,T}$ with $x \geq 0.87$ is obtained using the data of Baranowski et al. [30] at 25 °C and Burger et al. [34] at −77 °C. The expansion effect discussed above is considered in the calculation of $\rho'_{PdH_x,T}$ using the correction factor of the usual case. As a polynomial approximation, the data shown in Fig. 3(a) are fitted by the expression below:

$$10^2\rho'_{PdH_x,T}/\mu\Omega\ K^{-1} = 3.95 + 14.773x - 82.8x^2 + 219.632x^3 - 277.069x^4 + 126.826x^5 \quad (8)$$

with $R^2 = 0.9258$ and $\sigma^2 = 0.1478$. The resistivity ratio around T_R is:

$$\chi_\rho(T) = \frac{\rho_{PdH_x}(T_R) + \rho'_{PdH_x,T}(T - T_R)}{\rho_{Pd}(T_R) + \rho'_{Pd,T}(T - T_R)} \quad (9)$$

From Fig. 3(a), we find $\rho'_{PdH_x,T}$ exhibits complex behavior with x. The maximum value appears in the mixed α+β phase as was observed experimentally [3]: this can be interpreted by the percolation theory [40], i.e. $\rho'_{PdH_x,T}$ in the mixed α+β phase is greater than values in the α and β phases. This makes the maximum value of χ_ρ (or χ_R) flatten at high temperatures [20]. Because the α and β phases may have different profiles in a sample (see Section 3.4.2) and the phase boundary compositions x_α and x_β change with temperature, it is easy to understand that the data in this region are severely scattered. Another fact which has been neglected before is that $\rho'_{PdHx,T}$ in the high x region increases with x due to the optic-mode phonon of H in PdH_x, and this optic-mode contribution makes the resistivity of PdD greater than that of PdH as is shown in Fig. 1. Although the data in Fig. 3(a) are for hydrogen, deuterium shows an almost identical result according to Ref. [41].

A convenient quantity, widely used in experiments, is the temperature coefficient of resistance α_R defined as a dimensionless quantity [10,53,54]:

$$R_{PdH_x}(T) = R_{PdH_x}(T_R)[1 + \alpha_R(T - T_R)] \quad (10)$$

It is shown in Fig. 3(b) based on the same data in Fig. 3(a) [10,17,30,34]; the polynomial approximation to these data is:

$$10^3\alpha_R = 3.766 + 6.174x - 62.107x^2 + 190.596x^3 - 259.074x^4 + 125.51x^5 \quad (11)$$

with $R^2 = 0.98833$ and $\sigma^2 = 0.09656$. The resistance ratio around T_R can be normalized to that at room temperature:

$$\chi_R(T_R) = \frac{R_{PdH_x}(T)[1 - \alpha_R(T - T_R)]}{R_{Pd}(T_R)} \quad (12)$$

As experimentally, the temperature may change from time to time, the x value can be obtained by combining Eq. (12), the data of $\chi_R(T_R)$ and α_R by using the iterative method because α_R is also a function of x it is not necessary to find out $\chi_R(T)$. Another convenient way to determine x is by acquiring the resistance ratio of PdH_x at any temperature to Pd at T_R:

$$\chi_R(T,\ T_R) = \frac{R_{PdH_x}(T)}{R_{Pd}(T_R)} = \chi_R(T_R)[1 + \alpha_R(T - T_R)] \quad (13)$$

By plotting $\chi_R(T, T_R)$ at different temperatures, the x value can be obtained directly from these graphs. Of course, T_R in Eqs. (12) and (13) may not necessarily be 298.15 K in experiments; it can be any temperature as set initially.

Flanagan and Lewis [10] and Barton et al. [14] have studied $\chi_R(T)$ at $T = 0$–55 °C with $0 \leq x \leq 0.685$ and the corresponding χ_R has been used in past experiments [53,54]. The data of Flanagan and Lewis [10] are also shown in Fig. 3 (open squares). Because of the narrow range of temperature which induces χ_R changes of less than 5% and the inherent large error in the mixed α+β phase, the data are scattered and the relative error is significant.

3.3. Effect of hydriding–dehydriding cycles on the initial resistance of palladium

It is well known that if a Pd sample is hydrided and then dehydrided a number of times, i.e. 'cycled', the sample shape will deform strongly [1]. This deformation also affects the Pd resistance as was verified in our experiments and shown in Fig. 4. It is found that the R_{Pd} decreases almost linearly with the number of cycle. As a primary explanation, this effect can be understood by the dimensional changes during the hydriding–dehydriding cycles. Because self-stresses developed in a hydriding process are released by the expansion in the small size direction as discussed in Section 3.1 and this change is irreversible [3,69,79], the small size increases,

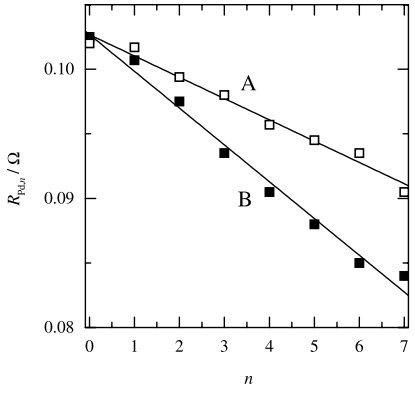

Fig. 4. Experimental results on the initial resistance of palladium after seven cycles of hydriding–dehydriding. The linear fit to results gives: $R_{Pd,n} = 0.1027(1-1.607\%\ n)\ \Omega$ and $0.1027(1-2.775\%\ n)\ \Omega$ for samples A and B, respectively. Both two samples are 0.02 cm in diameter and ca. 3 cm in length.

the large size decreases and the overall volume changes slightly after one cycle. For a sample with uniform cross-section S and length $l \gg S^{1/2}$, we have:

$$dV_{Pd} = l_{Pd}dS_{Pd} + S_{Pd}dl_{Pd} = 0 \quad (14)$$

in one cycle, where dV_{Pd}, dS_{Pd} and dl_{Pd} denote the changes of volume, cross-section and length of Pd sample after one hydriding–dehydriding cycle, respectively. We define the length change:

$$\gamma_l = -\frac{dl_{Pd}}{l_{Pd}} = \frac{dS_{Pd}}{S_{Pd}} \quad (15)$$

in one cycle, the length after n cycles is:

$$l_{Pd,n} = l_{Pd,0}\exp(-\gamma_l n) \quad (16)$$

Similarly, we obtain the resistance change after one cycle:

$$dR_{Pd} = \rho_{Pd}\left(\frac{dl_{Pd}}{S_{Pd}} - \frac{l_{Pd}dS_{Pd}}{S_{Pd}^2}\right) = -2\gamma_l R_{Pd} \quad (17)$$

Besides the dimensional changes, dislocations, cracks and voids are produced within the cycled sample [79–84], and these defects will cause an increase of the resistance although its magnitude is less than that caused by the dimensional change. To account for the overall effect on the resistance after one cycle, we use γ_R to replace $2\gamma_l$. Integrating Eq. (17) with respect to n, we obtain the Pd resistance after n cycles:

$$R_{Pd,n} = R_{Pd,0}\exp(-n\gamma_R) \quad (18)$$

If n is small this expression can be approximated by a linear function:

$$R_{Pd,n} = R_{Pd,0}(1 - n\gamma_R) \quad (19)$$

Experimental results are shown in Fig. 4 and we find that $\gamma_R = 1.61$ and 2.78% for samples A and B, respectively. Referring to the data in Ref. [68], the length of a Pd wire shrank from 609.144 to 585.154 mm after four cycles, which corresponds to $\gamma_l = 0.98\%$ from Eq. (16). Other similar data were obtained using a rectangular plate [80], the plate area of 6.0×2.5 cm^2 diminished to 1.12×0.53 cm^2 after 92 cycles and we obtain $\gamma_l = 1.82$ and 1.69% from Eq. (16). It can be proved that Eq. (16) is suitable for both cylindrical and rectangular shapes. These three sets of results are qualitatively consistent with each other and they indicate that the initial resistance must be measured after each cycle of hydriding–dehydriding. Even if the phase transition may not be complete in the hydrogen absorption-desorption processes, the initial electrode resistance also changes and its decrease depends on the extent of phase transition.

3.4. Effect of hydrogen concentration distribution on the PdH_x resistance ratio

In this subsection, we will discuss theoretically the effect of non-uniform distribution of hydrogen concentration in PdH_x on the sample resistance: we call it the non-uniform effect. Consider a measuring current flowing through a PdH_x sample with length l and uniform cross-section S, and the current direction is in the length direction. The non-uniform effect has two extreme situations in ISRM: one is that x changes in the direction perpendicular to length, e.g. a thin wire absorbs the hydrogen and the measuring current flows from one end to the other. The overall resistance is the parallel of those of thin layers in the length direction:

$$R_{PdH_x,p} = \left(\int \frac{dS}{\rho_{PdH_x} l}\right)^{-1} \quad (20)$$

We denote this situation as case p. Another extreme situation is that x changes only in the length direction, e.g. the concentration-cell effect induces x to change in the current direction as will be discussed afterwards. The total resistance is the series of those of thin layers perpendicular to the length direction:

$$R_{PdH_x,s} = \int \frac{\rho_{PdH_x} dl}{S} \quad (21)$$

We denote this situation as case s. Then, what we need to do is to discuss these two extreme situations: other complex cases are a mixture of these and the resistance is a value somewhere between $R_{PdH_x,p}$ and $R_{PdH_x,s}$.

Referring to Fig. 1, the regions of hydrogen concentration in the resistance graph can be divided into four parts: (1) the α phase; (2) the mixed α+β phase; (3) the β phase with x near x_{max} and (4) the β phase with x near 1. We will discuss the profile effect of these four aspects.

3.4.1. The α phase

For the α phase, it was found that:

$$\chi_R = 1 + A_1 x \quad (22)$$

with the coefficient $A_1 = 2.41$–3.7 for H [21–23] and 4.1 for D [11]. First, we discuss the non-uniform effect in case p. Combining Eqs. (1), (3), (4), (20) and (22) gives:

$$\chi_{R,p} = \chi_R(\bar{x}) - A_1^2\sigma^2 + O(\bar{x}^3) \quad (23)$$

with

$$\sigma^2 = \overline{(\bar{x}^2 - \bar{x}^2)} = \overline{(x - \bar{x})^2} \quad (24)$$

For simulating the practical case, we consider a cylindrical PdH_x sample with radius r_0 and length l which has been loaded with uniform hydrogen concentration x_0 as the initial value; the hydrogen concentration is switched to x_1 at $r = r_0$ and time $t = 0$. x at any time and place is [85]:

$$x = x_0 + (x_1 - x_0) \times \left(1 - 2\sum_{n=1}^{\infty} \frac{\exp(-\alpha_n^2 \tau_r) J_0(\alpha_n r/r_0)}{\alpha_n J_1(\alpha_n)}\right) \quad (25)$$

where α_n is the nth root of the Bessel function of the first kind of order zero, i.e. $J_0(\alpha_n) = 0$; r is the radial coordinate; $\tau_r = Dt/r_0^2$, is the reduced diffusion time in the radial direction, where D is the diffusion coefficient of H in Pd. Similarly to the deduction of Eq. (23), the effective resistance and the effective x value measured by ISRM can be obtained from Eq. (22). Fig. 5 shows an example of this situation with $x_0 = 0$ and $x_1 = 0.1$. The average hydrogen concentration at a time is [85]:

$$\bar{x} = x_0 + (x_1 - x_0)\left(1 - \sum_{n=1}^{\infty} \frac{4}{\alpha_n^2} \exp(-\alpha_n^2 \tau_r)\right) \quad (26)$$

$\bar{x}$ and the relative error are also shown in Fig. 5. We find that the maximum error appears in the initial period as expected.

For the case s, by combining Eqs. (1), (3), (4), (21) and (22), we have:

$$\chi_{R,s} = \chi_R(\bar{x}) \quad (27)$$

For simulating this situation, we consider that the cylindrical sample absorbs hydrogen at the two end faces; hydrogen atoms diffuse in the axial direction with the first boundary condition as discussed above. The hydrogen concentration at any time and place is [85]:

$$x = x_0 + (x_1 - x_0) \times \left\{1 - \frac{4}{\pi}\sum_{n=0}^{\infty} \times \frac{1}{2n+1} \sin\frac{(2n+1)\pi z}{l} \exp[-(2n+1)^2\pi^2\tau_l]\right\} \quad (28)$$

where z is the axial coordinate; $\tau_l = Dt/l^2$, is the reduced diffusion time in the axial direction. The resistance can be obtained by introducing this equation into Eqs. (1), (3), (4), (21) and (22), and the effective hydrogen concentration is obtained by solving Eq. (22). The average hydrogen concentration in this situation is [85]:

$$\bar{x} = x_0 + (x_1 - x_0) \times \left\{1 - \sum_{n=0}^{\infty} \frac{8}{(2n+1)^2\pi^2} \exp[-(2n+1)^2\pi^2\tau_l]\right\} \quad (29)$$

A related example is also shown in Fig. 5. In this case, the measured x is exactly the average value due to the linear nature of Eqs. (21) and (22).

For a general form of hydrogen distribution, the total resistance is between $R_{PdH_x,p}$ and $R_{PdH_x,s}$, so the relative error arising from the non-uniform effect is:

$$-A_1\frac{\sigma^2}{\bar{x}^2} \le \delta \le 0 \quad (30)$$

This result indicates that the measured hydrogen content is some less than the average value although the error is not substantial.

In this and the subsections below, we give examples of hydrogen diffusion only under the first boundary condition. It should be noted that actual situations are more complicated than here; the H concentration distribution depends on the bulk and surface properties of the electrode and the applied potential or current in electrochemical charging. However, the examples here give the limiting case because the surface process, which is always the rate-determining step, is very fast under the first boundary condition.

3.4.2. The α+β phase

For the mixed α+β phase, it has been verified by STM that the β phase is first formed near the outer surface of a Pd wire and the α→β phase transition accompanies the shrinkage of the α | β interface in the electrochemical charging process [57]. This means that the sample resistance can be seen as the parallel of the resistances of two single phases and the corresponding resistance ratio is:

$$\chi_{R,p} = \frac{\chi_{R,\alpha}\chi_{R,\beta}(x_\beta - x_\alpha)}{\chi_{R,\alpha}(x - x_\alpha) + \chi_{R,\beta}(x_\beta - x)} \quad (31)$$

where $\chi_{R,\alpha}$ and $\chi_{R,\beta}$ are the resistance ratios while $x = x_\alpha$ and x_β, respectively. If the two phases occupy different length regions, the overall resistance is the series of those in two singles phases:

$$\chi_{R,s} = \frac{\chi_{R,\alpha}(x_\beta - x) + \chi_{R,\beta}(x - x_\alpha)}{(x_\beta - x_\alpha)} \quad (32)$$

If the mixed α+β phase is composed of homogeneously dispersed granules of the α and β phases, the overall resistance can be seen as an appropriate average between the resistances of the pure α and β phases as

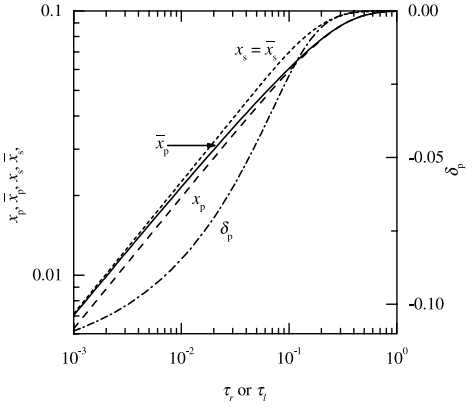

Fig. 5. Resistance ratio, average hydrogen concentration and relative error of the resistance method in the α phase during the diffusion process. The parameters: $x_0 = 0$, $x_1 = 0.1$, $A_1 = 2.41$.

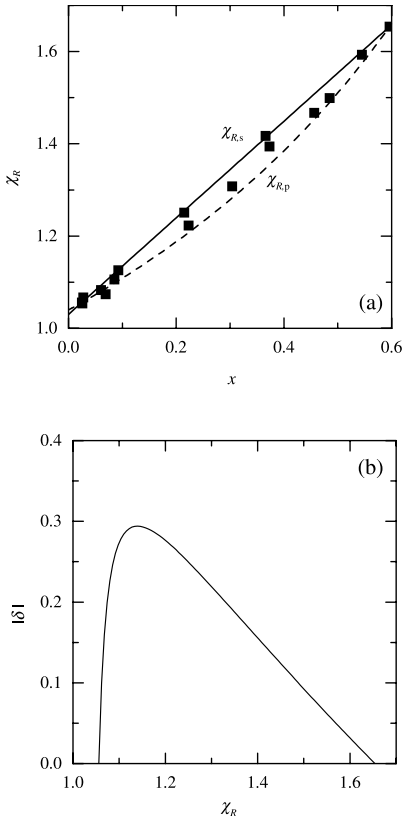

Fig. 6. (a) Resistance ratio of PdH_x in the mixed α+β phase, the scattered points are experimental results cited from Flanagan and Lewis [10] and the solid lines are theoretical results calculated from Eqs. (31) and (32); (b) the relative error in the mixed α+β phase. The parameters: $x_\alpha = 0.0247$, $x_\beta = 0.596$, $\chi_\alpha = 1.056$, $\chi_\beta = 1.654$.

interpreted by the percolation theory [40,43]. A comparison between the experiment results [10] and Eqs. (31) and (32) is illustrated in Fig. 6(a), where it is shown that the actual resistance ratio χ_R is between the values of $\chi_{R,p}$ and $\chi_{R,s}$. Generally speaking, in determining x by a given resistance ratio χ_R, we obtain the relative error by Eqs. (31) and (32):

$$|\delta| \le \frac{x_p - x_s}{\bar{x}} = \frac{2(x_p - x_s)}{x_p + x_s} = \frac{2(x_\beta - x_\alpha)(\chi_R - \chi_{R,\alpha})(\chi_{R,\beta} - \chi_R)}{(x_\beta - x_\alpha)(\chi_R^2 - \chi_{R,\alpha}\chi_{R,\beta}) + (x_\alpha + x_\beta)(\chi_{R,\beta} - \chi_{R,\alpha})\chi_R} \quad (33)$$

where x_p and x_s are the x values determined by Eqs. (31) and (32), respectively. Fig. 6(b) shows δ vs. x in the mixed α+β phase region. We find the maximum error can be as large as 30%, so in determining the hydrogen concentration one must be cautious. The above conclusion is obtained from the hydrogen absorption process, and can be applied to the hydrogen desorption process with the characteristic values in Eqs. (31)–(33) being replaced by the corresponding quantities in the β→α phase transition.

3.4.3. The β phase with x near x_{max}

When the resistance ratio is near the maximum value χ_{max}, its change with x can be expanded about the point x_{max} by a power series to the second order:

$$\chi = \chi_{max} - A_2(x - x_{max})^2 + O(x - x_{max})^3 \quad (34)$$

Similarly to the discussion in Section 3.4.1, we obtain the resistance ratio for both cases p and s:

$$\chi_{R,p} = \chi_{R,s} = \chi(\bar{x}) - A_2\sigma^2 \quad (35)$$

and the relative error is:

$$|\delta| \le \frac{A_2\sigma^2}{2|\bar{x} - x_{max}|} \quad (36)$$

This equation indicates that the measurement error will be much great when $\bar{x}$ is close to x_{max} or the concentration distribution is far from uniform. An example of case p is shown in Fig. 7, where the resistance is obtained by using Eqs. (1), (3), (4), (20) and (34). Contrary to the empirical expectation, the measured hydrogen concentration is quite different from the practical value especially when $\bar{x}$ nears x_{max} as shown by Eq. (36). This result also indicates that care is needed in the determination of hydrogen concentration around the maximum resistance region. In the numerical calculation, the diffusion coefficient is understood as the average value over a narrow range of hydrogen concentration because it actually changes with x in the β phase [86–88]. The case s is similar to the case p, so these results are not shown.

3.4.4. The β phase with x near 1

When x approaches 1, the resistance ratio decreases sharply with x. We can expand χ_R around the point $x = 1$ (stoichiometric palladium hydride):

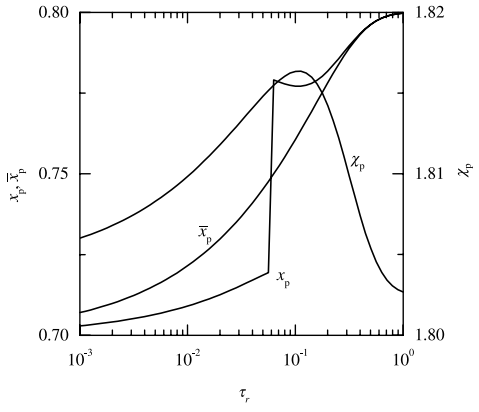

Fig. 7. Average hydrogen concentration $\bar{x}_p$, resistance ratio χ_p and the induced hydrogen content x_p in the hydrogen concentration region near x_{max} during hydrogen diffusion. The parameters: $\chi_{max} = 1.822$, $x_{max} = 0.75$, $A_2 = 7.5$, $A_3 = -6$ (for the convenience of determining x, the polynomial series in Eq. (34) is expanded to the third order), $x_0 = 0.7$ and $x_1 = 0.8$.

$$\chi_R = \chi_{R,\ \mathrm{PdH}} + A_1(1-x) - A_2(1-x)^2 + O(1-x)^3 \quad (37)$$

Similar to the above discussion, we obtain the resistance ratio for case p in the second order approximation:

$$\chi_\mathrm{p} = \chi(\bar{x}) - \left(A_2 + \frac{A_1^2}{\chi_\mathrm{PdH}}\right)\sigma^2 \quad (38)$$

and the resistance ratio for case s in the second order approximation:

$$\chi_\mathrm{s} = \chi(\bar{x}) - A_2\sigma^2 \quad (39)$$

The relative error under a general case is:

$$\frac{A_2\chi_\mathrm{PdH}}{A_1}\frac{\sigma^2}{\bar{x}} \le \delta \le \frac{A_2\chi_\mathrm{PdH} + A_1^2}{A_1}\frac{\sigma^2}{\bar{x}} \quad (40)$$

Fig. 8 shows numerical results based on Eqs. (1), (3), (4), (20), (21) and (37) for both cases. We find a substantial error appears only at the beginning, and the maximum error is less than 1%. These results are consistent with Eq. (40) and this indicates that the ISRM is effective in the high x region.

In a word, although the non-uniform distribution of x may induce some errors, the most prominent effects on the determination of x by ISRM mainly occur while $x_\alpha < x < x_\beta$ or x is near $x_{\max}$. These defects can be avoided by controlling the electrolysis current density (ecd) in the electrochemical hydrogen charging, e.g. the resistance can be treated as case p for the mixed $\alpha+\beta$ phase region while the ecd is high and the error will be very little in the phase region when small ecd steps are applied.

It seems that the expansion effect discussed in Section 3.1 is omitted in this section. Actually, it is shown that the contributions of the correction factor cancel each other out.

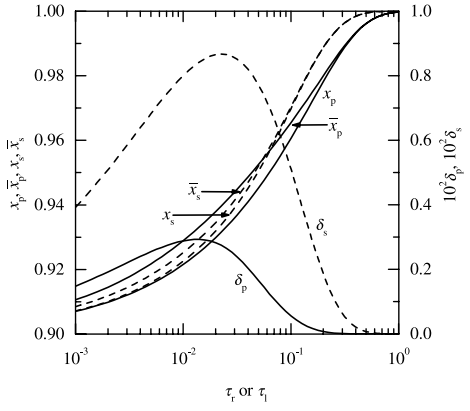

Fig. 8. Resistance ratio, average hydrogen concentration and relative error of the resistance method in the hydrogen concentration region near $x = 1$ during hydrogen diffusion. The parameters: $\chi_\mathrm{PdH} = 0.9325$, $A_1 = 7.665$ and $A_2 = 16.752$; $x_0 = 0.9$ and $x_1 = 1$.

3.5. Effect of electrolyte on the PdH_x resistance in the in situ measurement

In the ISRM of the PdH_x electrode, the surrounding electrolyte, the applied ec and the electrode configuration itself all influence the resistance measurements. First, the solution acts as a resistance in parallel with the electrode and the apparent PdH_x resistance is reduced when co-conduction is in progress. Second, the potential drop across the electrode induced by the measuring dc makes it behaves as a concentration-cell, which contributes an additional potential shift to the signal measured. Thirdly, the ec contributes another potential drop to the electrode by the current collection into the electrode and the concentration-cell effect. Finally, the lead electrode exposed to the electrolyte or other defects in the electrode configuration and design can influence the ISRM due to the concentration-cell effect. Although some of these factors have been studied experimentally [50–52], a detailed and complete consideration has been lacking up to now. In this and the subsections below, we will study these problems theoretically in turn. First of all, let us discuss the effect of the electrolyte solution on the ISRM.

3.5.1. Co-conduction of electrolyte

The co-conduction of the electrolyte can be seen as the resistance that is in parallel with the electrode. There are three configurations for an electrode with length l and radius r_0 as shown in Fig. 9 (a); the first is a straight rod, which we call shape I as it is in the shape of this letter and this was used in most previous experiments [52–57]. The second is a spiral electrode as used in the present work, which we call shape W. The third is an electrode bent in the shape of a letter U; the non-induction loop used in Refs. [49–51] is of this type. Other situations can be considered as a combination of

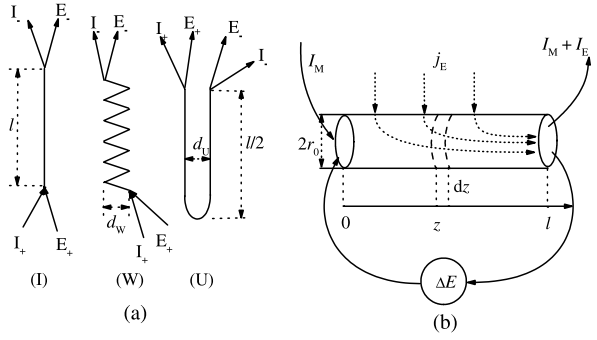

Fig. 9. Schematic diagram of a PdH_x wire electrode used in the resistance measurement. (a) Electrodes of shapes I, W and U, respectively; (b) the magnification representation of the electrode used in the measurement and electrolysis process. r_0 and l are radius and length of the electrode, respectively; I_M and I_E are the measurement and electrolysis currents in the z direction, respectively; electrolysis current density j_E is distributed uniformly on the electrode and is collected at $z = l$.

these. For the shape I, the solution resistance can be seen as the series resistance of two hemispheres with radius r_0; for the shape W, the resistance is equivalent to the series resistance of coaxial circles with diameter d_W that is much greater than r_0; for the shape U, the electrolyte resistance is equal to the resistance between two long parallel wires with length $l/2$, radius r_0 and distance $d_U \gg r_0$. Their resistances are easily obtained from a textbook of electromagnetics:

$$R_S = \frac{\rho_S}{\pi} \times \begin{cases} \dfrac{1}{r_0}, & \text{for shape I} \\ \dfrac{l}{\pi^2 d_W^2} \ln\dfrac{d_W}{r_0}, & \text{for shape W} \\ \dfrac{2}{l} \ln\dfrac{d_U}{r_0}, & \text{for shape U} \end{cases} \tag{41}$$

where ρ_S is the resistivity of solution. The additional resistance contribution to that of a PdH_x electrode by the co-conduction of the solution, $R_{A,S}$ can be expressed as:

$$\frac{R_{A,S}}{R_{PdH_x}} = -\frac{R_{PdH_x}}{R_S} = -\frac{\rho_{PdH_x} l}{R_S \pi r_0^2}$$

$$= -\frac{\rho_{PdH_x}}{\rho_S} \times \begin{cases} \dfrac{l}{r_0}, & \text{for shape I} \\ \dfrac{\pi^2 d_W^2}{r_0^2}\left(\ln\dfrac{d_W}{r_0}\right)^{-1}, & \text{for shape W} \\ \dfrac{l^2}{2r_0^2}\left(\ln\dfrac{d_U}{r_0}\right)^{-1}, & \text{for shape U} \end{cases} \tag{42}$$

For example, $l/r_0 = 10^2$, $d_W/r_0 = d_U/r_0 = 10$, $\rho_{PdH_x} = 10^{-5}$ Ω cm and $\rho_S = 10$ Ω cm and the amplitudes of $R_{A,S}/R_{PdH_x}$ are 10^{-4}, 4.3×10^{-4} and 2.2×10^{-3} for shapes I, W and U, respectively. From Eq. (42), we find that a long and/or thin electrode, good conduction of the solution will give a significant co-conduction effect as expected.

3.5.2. Concentration-cell effect in the resistance measurement

Knorr and Schwartz [47,48] and Carson et al. [49–51] have found that the apparent PdH_x resistance drifts upward to a larger value when a measuring dc passes through a sample immersed in electrolyte. This phenomenon can be interpreted by the concentration-cell effect [49–51]. When a potential difference is applied between the two ends of the electrode, the loss of hydrogen from the positive electrode will result in an electrode potential above 0 V and simultaneously the electrode potential of the negative electrode will correspondingly decrease below 0 V. Proton transfer ceases, apart from the leak current, when the potential developed between the two ends equals the applied potential. The final concentration of hydrogen in the electrode may be calculated from the available relationship between hydrogen content and electrode potential. At the same time, this polarization will contribute an additional potential fall, which makes the apparent resistance greater than the actual value. We will discuss this effect quantitatively below.

Consider a measurement current I_M passing through an electrode as shown in Fig. 9(b); the electromotive force (emf) of the concentration-cell is the potential drop $I_M R_{PdH_x}$, which is built up over a period time [50] and can be expressed as:

$$E_C = I_M R_{PdH_x}\left(\frac{1}{2} - \frac{z}{l}\right) \tag{43}$$

as shown in Fig. 10(a), where the fraction 1/2 in the parentheses ensures that the average potential is zero. The emf makes the hydrogen concentration in the electrode redistribute in the current direction. From the isotherm of hydrogen in the β phase PdH_x electrode [46,89,90], we have:

$$-FE = \mu_{H,0} + U_b x + RT \ln\left(\frac{x}{1-x}\right) \tag{44}$$

where $\mu_{H,0}$ is the chemical potential of hydrogen in the reference state, $U_b = 49$ kJ mol^{-1}, is the H–H interaction energy [46] and the other symbols have their usual meanings. We can obtain the concentration departure from the average value at a point by the differential of Eq. (44) with respect to potential:

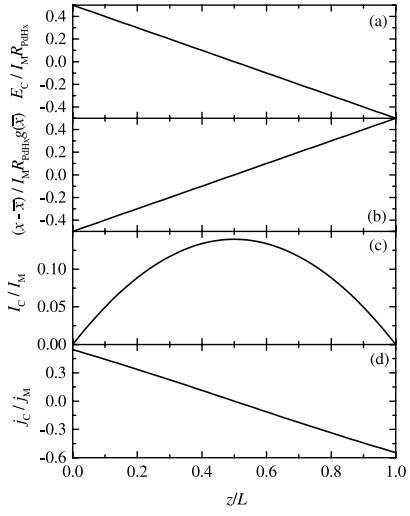

Fig. 10. The concentration-cell effect induced by the measurement current. (a) The potential distribution; (b) the hydrogen concentration distribution; (c) the current distribution and (d) the current density distribution in the PdH_x electrode in the current direction. $j_M = I_M/2\pi r_0 l$. Parameter: $k = 1$.

$$x = \bar{x} - g(\bar{x})E_C = \bar{x} + g(\bar{x})I_M R_{PdH_x}\left(\frac{z}{l} - \frac{1}{2}\right) \quad (45)$$

with

$$g(x) = f\left[\frac{U_b}{RT} + \frac{1}{(1-x)x}\right]^{-1} \quad (46)$$

and $f = F/RT$. The numerical example is shown in Fig. 10(b). Introducing Eq. (45) into Eq. (24) gives the standard deviation:

$$\sigma^2 = \frac{1}{12}\, g(\bar{x}) I_M R_{PdH_x} \quad (47)$$

For example, for $R_{PdH_x} = 10^{-1}\ \Omega$, $I_M = 10^{-1}$ A, $U_b/RT = 18.1$ and $\bar{x} = 0.7$, we obtain $\sigma^2 = 1.4 \times 10^{-3}$ which is much less than the average value, so the concentration redistribution does not induce any noticeable error as was concluded from the discussion in Section 3.4.

The overall emf is comprised of the ohmic potential drop of the external circuit (i.e. the PdH_x electrode itself) $\Delta E_{PdH_x,C}$, the ohmic polarization of the inner resistance (i.e. the electrolyte solution) $\Delta E_{S,C}$ and the electrochemical overpotential η_C. The potential drop across the small distance dz at point z in the PdH_x electrode is:

$$dE_{PdH_x,C} = -I_C R_{PdH_x}\, dz/l \quad (48)$$

The electrolyte resistance in the small distance dz can be seen as the resistance of a part of the cylindrical electrode with radius r_0 and surface area $2\pi r_0 dz$ in the solution for the shapes I and W or the resistance of two parallel electrodes with distance d_U and length dz for the shape U. These two situations can be treated individually as:

$$\Delta E_{S,C} = R_{S,C} l \frac{dI_C}{dz} \quad (49)$$

with

$$R_{S,C} = \frac{\rho_S}{2\pi l} \times \begin{cases} \ln\dfrac{l}{r_0}, & \text{for shapes I and W} \\ \ln\dfrac{d_U}{r_0}, & \text{for shape U} \end{cases} \quad (50)$$

$R_{S,C}$ is equivalent to the resistance between two parallel wires with length $4l$, radius r_0 and distance l for shapes I and W, or distance d_U for shape U. By comparison with Eq. (41), we find that $R_{S,C}$ is much less than R_S. Using the parameters in Section 3.5.1 and $l = 10$ cm, we obtain $R_{S,C} = 0.73\ \Omega$ for shapes I and W, and 0.37 Ω for shape U.

From the relationship between the overall ecd j_E and overpotential η on the Pd/H electrode [89,90], we obtain:

$$|j_E| \propto \begin{cases} j_{0V} f|\eta|, & \text{if } j_E \sim 0 \\ \exp(\beta f|\eta|), & \text{if } |j_E| \gg j_{0T} \end{cases} \quad (51)$$

where j_{0V} and j_{0T} are the exchange current densities of the Volmer and Tafel reactions, β is the stoichiometric number of the electrochemical reaction and it is connected with the Tafel slop b by the relation $b = 2.303/\beta f$. The symbol of the absolute value in this equation ensures that the anodic and cathodic processes are expressed by a unified form. Eq. (51) is more empirical than fundamental because the actual overpotential-ecd relation is complex [89,90]. In general, β is between 0 and 2 and its value depends on the mechanism of the electrode reaction. For the hydrogen evolution reaction (her), $\beta = 2$ when the reaction follows the fast Volmer–slow Tafel mechanism, $\beta = 1/3$ when the reaction follows the coupled Volmer–Tafel mechanism and $\beta = 0$ when the ecd approaches the limiting value. For the anodic oxide reaction, $0 < \beta < 2$ [89]. In this paper, the sign of j_E is determined by the direction of the ec relative to the measuring dc in the electrode as shown in Fig. 9(b). If they are in the same direction (i.e. $I_E/I_M > 0$), $j_E > 0$; otherwise, $j_E < 0$ while $I_E/I_M < 0$. This choice of sign differs from the conventional treatment where the positive and negative ecds are for the anodic and cathodic processes, respectively.

The overpotential of the concentration-cell can be obtained by the differential of the ecd with respect to η:

$$j_C = \frac{dj_E}{d\eta}\,\eta_C = j_{0C} f \eta_C \quad (52)$$

with the current density of the concentration-cell

$$j_C = \frac{dI_C}{2\pi r_0 dz} \quad (53)$$

and

$$j_{0C} = \begin{cases} j_{0V}, & \text{if } j_E \sim 0 \\ \beta|j_E|, & \text{if } |j_E| \gg j_{0T} \end{cases} \quad (54)$$

The potential at point z is the sum of the above three terms:

$$I_M R_{PdH_x}\left(\frac{1}{2} - \frac{z}{l}\right) = \left(\frac{1}{2\pi r_0 j_{0C} f} + R_{S,C} l\right)\frac{dI_C}{dz} + \int_0^Z I_C R_{PdH_x} dz/l \quad (55)$$

This equation can be simplified to an ordinary differential equation of second order:

$$l^2 \frac{d^2 I_C}{dz^2} + k^2 I_C = -k^2 I_M \quad (56)$$

with

$$k^2 = \frac{R_{PdH_x}}{R_C} \tag{57}$$

$$R_C = R_{S,C} + R_{\eta,C} \tag{58}$$

and

$$R_{\eta,C} = \frac{1}{2\pi r_0 l f j_{0C}} \tag{59}$$

The effective internal resistance R_C is composed of two terms: one is the resistance of solution, $R_{S,C}$, as shown in Eq. (50) and the other is the polarization resistance, $R_{\eta,C}$. The polarization resistance depends on the exchange current density of the Volmer reaction and the ecd as shown in Eq. (54). When j_E is great enough the polarization resistance will be very small. Applying the boundary condition:

$$I_C = 0 \quad \text{at } z = 0 \text{ and } l \tag{60}$$

we obtain the solution of Eq. (56):

$$I_C = \left[(1-\cos k)\frac{\sin\left(k\frac{z}{l}\right)}{\sin k} - \left(1-\cos\left(k\frac{z}{l}\right)\right)\right] I_M \tag{61}$$

and the current density of the concentration-cell from Eq. (53):

$$j_C = \left[(1-\cos k)\frac{\cos\left(k\frac{z}{l}\right)}{\sin k} - \sin\left(k\frac{z}{l}\right)\right] k j_M \tag{62}$$

with

$$j_M = \frac{I_M}{2\pi r_0 l} \tag{63}$$

Of course, the definition j_M has only a formal meaning. The potential drop contributed to the PdH_x electrode is:

$$\Delta E_{PdH_x,C} = \frac{1}{l}\int_0^l I_C R_{PdH_x} dz = h(k) I_M R_{PdH_x} \tag{64}$$

with the definition of $h(k)$ and its series expansion to the fourth order

$$h(k) = \frac{2}{k}\tan\frac{k}{2} - 1 = \frac{1}{12}k^2 + \frac{1}{120}k^4 + O(k^6), \tag{65}$$

while $k \ll 1$

It is 0.0926 for the parameter in Fig. 10. The additional resistance contributed to the original value induced by the measuring dc is:

$$R_{A,M} = h(k) R_{PdH_x} \tag{66}$$

Referring to Eqs. (50), (54), (58), (59), (65) and (66), we find there are many factors that can influence R_{PdH_x}/R_C and hence $R_{A,M}$. The first factor as usually expected is the conduction of the electrolyte; a high conduction of electrolyte results in small $R_{S,C}$ and R_C (see Eqs. (50) and (58)), and a large $R_{A,M}$ as is observed experimentally [50]. Contrary to one's expectation, the size, configuration and surface properties of the electrode also affect $R_{S,C}$, R_C and $R_{A,M}$, e.g. a long wire induces a large value of $R_{A,M}$ and this is one of the reasons for the high value of $R_{A,M}$ observed by Carson et al. [50] although they had not predicted it. An electrode with a rough surface results in a large value of j_{0V}, hence large values of j_{0C}, small values of R_C and high values of $R_{A,M}$ (see Eqs. (54), (58) and (65)). At the same time, some additives such as H_2S and thiourea can inhibit the reaction rate of the Pd/H electrode, so it is easy to understand that they can diminish $R_{A,M}$ as is observed experimentally [50]. Another factor is the ecd; a large ecd results in high values of j_{0C} and $R_{A,M}$ similar to the effect of j_{0V}. Because the ecd will induce an additional resistance as will be discussed in the subsection below, the effect of the ecd on the ISRM is more complex than expected.

On the other hand, if the electrode radius is very small or the length is very large, l/r_0 will be very great and the co-conduction of the solution will be substantial as is shown in Eq. (42). In this case, the effects of the electrolyte solution will be complicated. First, the co-conduction reduces the measurement resistance and hence the potential drop across the electrode. Second, the concentration-cell effect will be noticeable and the apparent resistance should be greater than the actual value. Therefore, this situation should be avoided in experiments.

The above discussion is suitable only if the measuring current is not high enough; otherwise, the hydrogen gas produced at the negative end cannot convert to atomic hydrogen at the positive end and the system is not reversible as was observed experimentally [50].

3.6. Effect of electrolysis current on resistance measurement

It is well known that the electrolysis process will disturb the electrode resistance measurement when the dc method is used [52]. To cancel this interference, a delta-mode current has been used to eliminate the deviation [52,54]. In this subsection we will discuss two aspects of the potential drop and additional resistance caused by the ec: one is that every electrode also acts as a current collector and hence bears a potential fall in the electrolysis process; the other is the concentration-cell effect induced by this potential shift.

3.6.1. Potential drop caused by the electrolysis current

In the ISRM of the electrode in the electrolysis process, the ec that is collected in the electrode will

contribute a potential drop to the measuring signal because the electrode has a resistance (see Fig. 9(b)). As a first approximation [91], we suppose that the ec (I_E) is uniformly distributed on the electrode. From a small distance dz at a point z as shown in Fig. 9(b), we obtain the relationship between the increment of current in the electrode and j_E:

$$dI_{PdH_x,E} = 2\pi r_0 j_E dz \tag{67}$$

where the ecd j_E is related to I_E by:

$$j_E = \frac{I_E}{2\pi r_0 l} \tag{68}$$

The potential drop across the small distance dz is:

$$dE_{PdH_x,E} = -\frac{R_{PdH_x}}{l} I_E dz \tag{69}$$

Combining these three equations and integrating $dE_{PdH_x,E}$ with respect to z, we obtain the potential at a point z caused by the electrolysis current collection:

$$E_{PdH_x,E} = \frac{I_E R_{PdH_x}}{2}\left(\frac{1}{3} - \frac{z^2}{l^2}\right) \tag{70}$$

as shown in Fig. 11(a), where the fraction 1/3 in the parentheses ensures that the average potential is zero. The corresponding potential drop across the electrode is:

$$\Delta E_{PdH_x,E} = \frac{I_E R_{PdH_x}}{2} \tag{71}$$

This means that the electrode behaves as that with a half value of the original resistance.

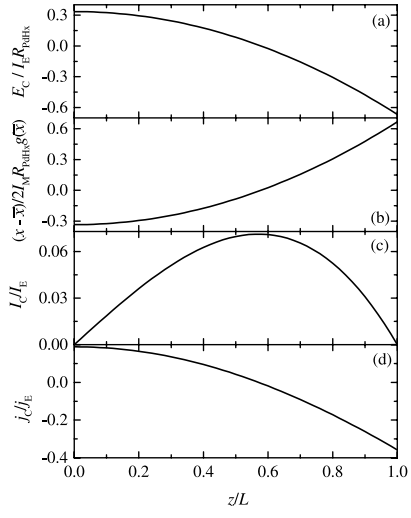

Fig. 11. The concentration-cell effect induced by the electrolysis current. (a) The potential distribution; (b) the hydrogen concentration distribution; (c) the current distribution and (d) the current density distribution in the PdH_x electrode in the current direction. Parameter: $k = 1$.

Of course, the above conclusion is appropriate only when the ecd is uniformly distributed in the length direction (but radial symmetry need not be applied, in a general situation, $2\pi r_0$ in Eq. (68) should be replaced by the rod perimeter); this assumption is difficult to preserve when H_2 bubbles are produced and the ecd increases in the her [92,93]. However, $\Delta E_{PdH_x,E}$ must not be greater than IR_{PdH_x} which means that the ec is so non-uniform that it is concentrated only at one end.

3.6.2. Concentration-cell effect caused by the electrolysis current

Because the ec contributes a potential drop between the ends of electrode, it also has a concentration-cell effect as discussed in Section 3.5.2. First, we give the hydrogen concentration departure from the uniform distribution by replacing E_C in Eq. (45) with $E_{PdH_x,E}$ in Eq. (70):

$$x = \bar{x} + \frac{I_E R_{PdH_x} g(\bar{x})}{2}\left(\frac{z^2}{l^2} - \frac{1}{3}\right) \tag{72}$$

with $g(x)$ defined in Eq. (46), the hydrogen distribution is shown in Fig. 11(b). Introducing Eq. (72) into Eq. (24) gives the standard deviation:

$$\sigma^2 = \frac{2}{45} g(\bar{x}) I_E R_{PdH_x} \tag{73}$$

For example for $I_E = 10^{-1}$ A and other parameters being the same as in the discussion of Eq. (47), we have $\sigma^2 = 7.5 \times 10^{-4}$ which is much less than $\bar{x}$.

Similarly to Eq. (56), we obtain an ordinary differential equation of second order:

$$l^2 \frac{d^2 I_C}{dz^2} + k^2 I_C = -k^2 I_E \frac{z}{l} \tag{74}$$

The solution is:

$$I_C = \left[\frac{\sin\left(k\frac{z}{l}\right)}{\sin k} - \frac{z}{l}\right] I_E \tag{75}$$

and

$$j_C = \left[\frac{k\cos\left(k\frac{z}{l}\right)}{\sin k} - 1\right] j_E \tag{76}$$

The potential shift contributed to the external circuit is:

$$\Delta E_{PdH_x,C} = \frac{1}{2} h(k) I_E R_{PdH_x} \tag{77}$$

The corresponding additional resistance contributed to the measurement value is the sum of these resistances caused by the electrolysis current collection and its

concentration-cell effect as shown in Eqs. (71) and (77):

$$R_{A,E} = \frac{I_E}{2I_M}[1 + h(k)]R_{PdH_x} \quad (78)$$

From this equation, it is found that the contribution of the electrolysis process to the ISRM depends on the direction and magnitude of the ec in addition to the factors discussed in Section 3.5.2. If the ec is in the direction of the measuring dc in the PdH_x electrode, i.e. $I_E/I_M > 0$, it will contribute another positive shift besides $R_{A,M}$ to the measured resistance. Otherwise, it will diminish the magnitude of the measured value when $I_E/I_M < 0$. In experiments, its influence can be avoided through an appropriate choice of the measuring current. If the measuring current is much greater than the ec, $R_{A,E}$ will be $\ll R_{A,M}$ and $R_{A,E}$ can be omitted. On the other hand, we can use the delta-mode current; i.e. at time $t1$ for the positive current and at $t2$ for the negative current, the compensated value $(V_{t1} - V_{t2})/2$ ensures that the true value is readily displayed. The current direction changes periodically and this delta mode can be programmed using the front panel controls. Of course, the magnitude of I_M must not be much less than I_E in this case; otherwise, the error will be very marked because $(V_{t1} - V_{t2})/2$ is a subtraction of two large numbers, V_{t1} and V_{t2}.

It must be pointed out that $\Delta E_{PdH_x,E}$ appears instantly when the ec is applied, whereas $\Delta E_{PdH_x,C}$ is delayed by a time interval which depends on the electrode diameter and surface properties [49–51].

The above deduction is for the perfect electrode. In the practical case there are two factors causing the results to depart from the ideal value. One is that the electrode resistance R_{PdH_x} is of the same order as the solution resistance R_S; the ecd on electrode is non-uniform and it changes with position as discussed in Ref. [91]. The other is that H_2 gas bubbles produced on the erect PdH_x electrode in the her make the ecd in the bottom region greater than that in the top region, hence the non-uniformity of the ecd increases. These two situations make the magnitude of $R_{A,E}$ differ from, but not go beyond twice the value of $R_{A,E}$ in Eq. (78). Because the extremely inhomogeneous cases are that the overall ec passes from one end to the other, as does the measuring current, or only passes through one end, so we have:

$$0 \le |R_{A,E}| \le \left|\frac{I_E}{I_M}\right|[1 + h(k)]R_{PdH_x} \quad (79)$$

When the ecd is very high, the volume and number of H_2 bubbles adhering to the PdH_x surface will be so numerous that bubbles are positioned closer and finally interfere with each other and impede the solution contact with the electrode. The system becomes electrically unstable since no definite potential can be linked to the ecd [92,93], and the stable emf of the concentration-cell cannot be established in this case, hence $\Delta E_{PdH_x,E}$ changes at random. In experiments, stirring the solution around the electrode will enhance the mass transfer in the electrolyte and minimize the effect of bubbles. However, the usual method for enhancing the mass transfer, such as the rotating disc electrode, cannot be used because its technique requirements contradict those of the ISRM.

3.7. Concentration-cell effect caused by the imperfect configuration of the electrode

In addition to the potential drops caused by the applied currents as discussed in Sections 3.5 and 3.6, another similar concentration-effect arises from the imperfect configuration of the electrode. There may be two cases: (1) a PdH_x electrode acts as the anode and its one or more leads exposed to the electrolyte as the cathode form a concentration-cell; (2) one end of the electrode exposed to the gas may behave as drainage for preserving the fugacity of hydrogen in the electrode; the hydrogen concentration in the electrode near the electrolyte surface is then less than the average value and the electrode itself forms a concentration-cell. All these concentration differences may induce an emf:

$$\Delta E_C = \Delta x / g(\bar{x}) \quad (80)$$

where Δx is the hydrogen concentration difference between the PdH_x electrode and its equilibrium value for case (1), or the concentration difference exists in the PdH_x electrode itself in case (2). Similarly to Eqs. (64) and (77), we obtain the additional potential drop:

$$\Delta E_{PdH_x,C} = S_C h(k) \Delta E_C \quad (81)$$

where S_C is a shape factor of the order of 1 and its value depends on the geometrical characteristics of the electrode and its leads. The induced additional resistance is:

$$R_{A,I} = \pm \frac{S_C h(k) x}{g(\bar{x}) I_M} R_{PdH_x} \quad (82)$$

The sign of $R_{A,I}$ depends on which lead(or leads) and its (or their) area exposed to the electrolyte. Using the parameters: $\Delta x = 0.3$, $\bar{x} = 0.7$, $I_M = 0.1$ A, $R_{PdH_x}/R_C = 1$, it is about $\pm 0.163\ S_C R_{PdH_x}$, so it is important to avoid these defects in experiments.

Combining Eqs. (42), (66), (78) and (82), we obtain the apparent resistance in the ISRM during the electrolysis process:

$$R_{PdH_x,appa} = R_{PdH_x} + R_{A,S} + R_{A,M} + R_{A,E} + R_{A,I} = \left[\left(1+\frac{1}{2}\frac{I_E}{I_M}\right)(1+h(k)) - \frac{R_{PdH_x}}{R_S} \pm \frac{S_C h(k) x}{g(\bar{x}) I_M}\right] R_{PdH_x} \quad (83)$$

From this equation, we find that four measurement errors with different origins can be incorporated into a more uniform expression. On the whole, two ratios, i.e. I_E/I_M and R_{PdH_x}/R_S have the most important influence on the resistance measurement as was discussed above.

On the other hand, we can obtain the condition below from Eq. (83) for a perfect electrode ($R_{A,I} = 0$):

$$I_E = -2I_M\left[1 - \frac{R_{PdH_x}}{R_S} + \frac{1}{12}\frac{R_{PdH_x}^2}{R_S R_C}\right] \quad (84)$$

as a first approximation. The contributions of $R_{A,S}$, $R_{A,M}$ and $R_{A,E}$ cancel each other out, and the measured resistance is exactly the actual value. This means one can modify the measuring current during the electrolysis process to minimize the error. Because R_C depends on I_E according to Eq. (54), so Eq. (84) is not a strict linear function as expected, but it provides a suggestion for diminishing the measurement error in the ISRM.

The concentration-cell effect appears only in the single phase PdH_x electrode. In the mixed $\alpha+\beta$ phase, the chemical potential of hydrogen does not change in PdH_x under the external potential drop [50,51]. The apparent resistance is:

$$R_{PdH_x,appa} = \left(1+\frac{1}{2}\frac{I_E}{I_M} - \frac{R_{PdH_x}}{R_S}\right) R_{PdH_x} \quad (85)$$

Even in this case, the electrolysis current collection and electrolyte co-conduction still make contributions to the ISRM, so a low value of I_E/I_M is a necessary condition in the dc method.

The results of Sections 3.5, 3.6 and 3.7 are mainly theoretical and their qualitative aspects are consistent with available experimental results [47–52,54]. Their quantitative verification needs to be carried out in future experimental work.

4. Conclusions

In this paper, some problems on the resistance method in determining the hydrogen content in PdH_x electrodes are discussed. First, the resistivity ratio, the temperature coefficient of resistance and resistivity, and the resistance of palladium subjected to hydriding–dehydriding cycles are discussed. It is found that the resistivity ratio is somewhat higher than the resistance ratio for the same x value and its magnitude depends on the self-stress state caused by hydrogen insertion. The temperature coefficient increases with x when $x > 0.7$ which was omitted in previous work. The Pd resistance decreases with the number of hydriding–dehydriding cycles. Second, the effect of the inhomogeneous distribution of x in the electrode on determining the hydrogen content is discussed theoretically. It is proved that the errors are particularly significant when the Pd+H system is in the mixed $\alpha+\beta$ phase or when the resistance is near the maximum value. Finally, we discuss the additional potential shift and hence the apparent resistance of the PdH_x electrode caused by the co-conduction of the electrolyte, the concentration-cell effect and collection of the electrolysis current and imperfections of the electrode configuration in the ISRM. The quantitative expression of these effects is given and some of the theoretical predications are consistent with available experimental results. Some advice is given for measuring the resistance in experiments.

5. List of symbols

A_i	ith expansion coefficient in a polynomial series
b	Tafel slope
D	diffusion coefficient of H in Pd
d_U	distance between two electrodes of shape U shown in Fig. 9(a)
d_W	diameter of an electrode of shape W shown in Fig. 9(a)
f	$= F/RT$
$g(x)$	defined in Eq. (46)
$h(k)$	defined in Eq. (65)
I_i	current of i (i = C, E and M)
J_n	Bessel function of nth order
j	current density
j_{0V}	exchange current density of the Volmer reaction in the hydrogen electrode reaction
j_{0T}	exchange current density of the Tafel reaction in the hydrogen electrode reaction
j_{0C}	effective exchange current density defined in Eq. (54)
k	defined in Eq. (57)
l	length of PdH_x electrode
l_{Pd}	length of Pd electrode
n	cycle number of palladium hydriding–dehydriding
R	universal gas constant
R^2	correlation coefficient
R_i	resistance of substance i
r	radial coordinate
r_0	radius of PdH_x electrode
S	cross-section of PdH_x electrode
S_C	shape factor of the concentration-cell defined in Eq. (81)
S_{Pd}	cross-section of Pd electrode

t time
T temperature
T_R = 298.15 K, room temperature
U_b H–H interaction energy in PdH_x
V volume
x atom ratio of H to Pd
x_0 initial value of x
x_1 boundary value of x
z axial coordinate

Greek symbols

α_n nth root of the Bessel function of the order of zero
α_R temperature coefficient of resistance of PdH_x
β stoichiometric number of electrochemical reaction of Pd/H electrode.
χ_R resistance ratio of palladium hydride to palladium
χ_ρ resistivity ratio of palladium hydride to palladium
δ relative error
ε expansion factor
ε_R correction factor defined in Eq. (7)
γ_l length change in one cycle of the hydriding–dehydriding process
γ_R resistance change in one cycle of the hydriding–dehydriding process
η overpotential
ρ resistivity
σ^2 standard deviation
τ_r $= Dt/r_0^2$, reduced diffusion time in the radial direction
τ_l $= Dt/l^2$, reduced diffusion time in the axial direction
$\mu_{H,0}$ hydrogen chemical potential in the reference state

Subscripts

A additional (resistance)
appa apparent (resistance)
C concentration-cell
E electrolysis process
I imperfect configuration of electrode
l length
M measurement
max maximum (resistance)
n cycle number of the palladium hydriding–dehydriding process
p (resistance) in parallel
Pd palladium electrode
PdH_x PdH_x electrode
PdH electrode of the stoichiometric palladium hydride
R resistance
S solution
s (resistance) in series
T temperature
V volume
α boundary value of α phase in the mixed α+β phase
β boundary value of β phase in the mixed α+β phase
ρ resistivity

Superscripts etc.

′ differential
¯ average value

Acknowledgements

This work was supported by NSFC No. 10145006 & 20103009 and the President's Innovation Foundation in Chinese Academy of Sciences. We wish to acknowledge the assistance of Master J. Gu who designed and carried out some of experiments.

References

[1] F.A. Lewis, The Palladium Hydrogen System, Academic Press, London, 1967, p. 50.
[2] F.A. Lewis, Plat. Met. Rev. 26 (1982) 20.
[3] F.A. Lewis, Plat. Met. Rev. 26 (1982) 70.
[4] B. Baranowski, in: G. Alefeld, J. Völkl (Eds.), Hydrogen in Metals II, Application-Oriented Properties, Topics in Applied Physics, vol. 29, Springer, Berlin, 1978, p. 157.
[5] F. Fischer, Ann. Phys. 20 (1906) 503.
[6] H. Brüning, A. Sieverts, Z. Phys. Chem. A 163 (1933) 409.
[7] H. Hagen, A. Sieverts, Z. Phys. Chem. A 165 (1933) 1.
[8] A. Sieverts, W. Danz, Z. Phys. Chem. B 38 (1938) 61.
[9] T.B. Flanagan, F.A. Lewis, Trans. Faraday Soc. 55 (1959) 1400.
[10] T.B. Flanagan, F.A. Lewis, Z. Phys. Chem. (N.F.) 27 (1961) 104.
[11] T.B. Flanagan, J. Phys. Chem. 65 (1961) 280.
[12] J.C. Barton, F.A. Lewis, Z. Phys. Chem. (N.F.) 33 (1962) 99.
[13] J.C. Barton, F.A. Lewis, Trans. Faraday Soc. 58 (1962) 103.
[14] J.C. Barton, F.A. Lewis, I. Woodward, Trans. Faraday Soc. 59 (1963) 1201.
[15] J.C. Barton, W.F.N. Leitch, F.A. Lewis, Trans. Faraday Soc. 59 (1963) 1208.
[16] F.A. Lewis, W.D. McFall, T.C. Witherspoon, Z. Phys. Chem. (N.F.) 114 (1979) 239.
[17] R.-A. McNicholl, F.A. Lewis, Z. Phys. Chem. (N.F.) 181 (1993) 239.
[18] F.A. Lewis, K. Kandasamy, R.-A. McNicholl, X.Q. Tong, Int. J. Hydrogen Energy 20 (1995) 369.
[19] P. Wright, Proc. Phys. Soc. A 63 (1950) 727.
[20] P.L. Levine, K.E. Weale, Trans. Faraday Soc. 56 (1960) 357.
[21] W.T. Lindsay, F.W. Pement, J. Chem. Phys. 36 (1962) 1229.
[22] K. Baba, U. Miyagawa, K. Watanabe, Y. Sakamoto, T.B. Flanagan, J. Mater. Sci. 25 (1990) 3910.
[23] Y. Sakamoto, F.L. Chen, M. Kinoshita, M. Minamikawa, J. Alloy. Compd. 192 (1993) 141.
[24] Y. Sakamoto, K. Takai, I. Takashima, M. Imada, J. Phys.: Condens. Mater 8 (1996) 3399.
[25] A.K.M.F. Kibria, Y. Sakamoto, Int. J. Hydrogen Energy 23 (1998) 475.

[26] A.K.M.F. Kibria, T. Tanaka, Y. Sakamoto, Int. J. Hydrogen Energy 23 (1998) 891.
[27] B. Baranowski, R. Wiśniewski, J. Phys. Chem. Solids 29 (1968) 1275.
[28] B. Baranowski, R. Wiśniewski, Phys. Status Solidi 35 (1969) 593.
[29] A.W. Szafranski, B. Baranowski, Phys. Status Solidi A 9 (1972) 435.
[30] B. Baranowski, F.A. Lewis, W.D. McFall, S.M. Filipek, T.C. Witherspoon, Proc. Roy. Soc. London A 386 (1983) 309.
[31] B. Baranowski, S.M. Filipek, J. Less-Comm. Met. 158 (1990) 347.
[32] G. Bamkakidis, R.J. Smith, D.A. Otterson, Phys. Rev. 177 (1969) 1044.
[33] R.J. Smith, D.A. Otterson, J. Phys. Chem. Solids 31 (1970) 187.
[34] J.P. Burger, D.S. MacLachlan, R. Mailfert, B. Souffaché, Solid State Commun. 17 (1975) 277.
[35] D.S. MacLachlan, R. Mailfert, J.P. Burger, Solid State Commun. 17 (1975) 281.
[36] J.P. Burger, S. Senoussi, B. Soufaché, J. Less-Comm. Met. 49 (1976) 213.
[37] J.P. Burger, J. Less-Comm. Met. 130 (1987) 1.
[38] M. Nicolas, H. Raffy, L. Dumoulin, J.P. Burger, J. Less-Comm. Met. 130 (1987) 61.
[39] D.S. MacLachlan, J.P. Burger, Solid State Commun. 65 (1988) 159.
[40] J.P. Burger, Z. Phys. Chem. (N.F.) 179 (1993) 365.
[41] N.S. Ho, F.D. Manchester, Can. J. Phys. 46 (1968) 1341.
[42] C.T. Haywood, L. Verdini, Can. J. Phys. 46 (1968) 2065.
[43] R. Fletcher, N.S. Ho, F.D. Manchester, J. Phys. C: Solid State Phys. 3 (1970) S59.
[44] G.A. Frazier, R. Glosser, J. Less-Comm. Met. 74 (1980) 89.
[45] M.-W. Lee, R. Glosser, Z. Phys. Chem. (N.F.) 147 (1986) 27.
[46] E. Wicke, G.H. Nernst, Ber. Bunsenges. Phys. Chem. 68 (1964) 224.
[47] C.A. Knorr, E. Schwartz, Z. Elektrochem. 39 (1933) 281.
[48] C.A. Knorr, E. Schwartz, Z. Elektrochem. 40 (1934) 36.
[49] A.W. Carson, T.B. Flanagan, F.A. Lewis, Naturwiss 46 (1959) 374.
[50] A.W. Carson, T.B. Flanagan, F.A. Lewis, Trans. Faraday Soc. 56 (1960) 1311.
[51] A.W. Carson, T.B. Flanagan, F.A. Lewis, Trans. Faraday Soc. 56 (1960) 1324.
[52] D.J. Gillespie, G.N. Kamm, A.C. Ehrlich, P.L. Mart, Fusion Technol. 16 (1989) 526.
[53] M.C.H. McKubre, S. Crouch-Baker, R.C. Rocha-Filho, S.I. Smedley, F.L. Tanzella, T. Passell, J. Santucci, J. Electroanal. Chem. 368 (1994) 55.
[54] T.A. Green, T.I. Quickenden, J. Electroanal. Chem. 368 (1994) 121.
[55] A. Wark, S. Crouch-Baker, M.C.H. McKubre, F.L. Tanzella, J. Electroanal. Chem. 418 (1996) 199.
[56] A. De Ninno, A. La Barbera, V. Violante, J. Alloy. Compd. 253–254 (1997) 181.
[57] T. Senjuh, H. Kamimura, T. Uehara, M. Sumi, S. Miyasita, T. Sigemitsu, N. Asami, J. Alloy. Compd. 253–254 (1997) 617.
[58] L.E.A. Berlouis, P.J. Hall, A.J. MacKinnon, A.W. Wark, D. Manuelli, V. Gervais, J.E. Robertson, J. Alloy. Compd. 253–254 (1997) 207.
[59] A. Czerwiński, I. Kiersztyn, M. Grdeń, J. Czapla, J. Electroanal. Chem. 471 (1999) 190.
[60] A.M. Riley, J.D. Seader, D.W. Pershing, C. Walling, J. Electrochem. Soc. 139 (1992) 1342.
[61] R. Felici, L. Bertalot, A. De Ninno, A. La Barbera, V. Violante, Rev. Sci. Instrum. 66 (1995) 3344.
[62] A.E. Munter, B.J. Heuser, Phys. Rev. B 58 (1998) 678.
[63] M.R. Hawkesworth, J. Electroanal. Chem. 119 (1981) 49.
[64] B. Baranowski, S. Majchrzak, T.B. Flanagan, J. Phys. F: Met. Phys. 1 (1971) 258.
[65] J.E. Schirber, B. Morosin, Phys. Rev. B 12 (1975) 117.
[66] H.C. Jamieson, G.C. Weatherly, F.D. Manchester, J. Less-Comm. Met. 50 (1976) 85.
[67] T.B. Flanagan, B.S. Bowerman, G.E. Biehl, Scr. Metall. 14 (1980) 443.
[68] T. Graham, Proc. Roy. Soc. London 17 (1869) 212.
[69] F.M. Mazzolai, P.G. Bordoni, F.A. Lewis, J. Phys. F 11 (1981) 337.
[70] D.P. Smith, Hydrogen in Metals, University of Chicago Press, Chicago, IL, 1948, p. 247.
[71] B. Stritzker, W. Buckel, Z. Phys. 257 (1972) 1.
[72] B. Stritzker, H. Wühl, in ref. 4, p. 243
[73] T. Skośkiewicz, Phys. Status Solidi A 11 (1972) K123.
[74] T. Skośkiewicz, A.W. Szafrański, W. Bujnowski, B. Baranowski, J. Phys. C: Solid State Phys. 7 (1974) 2670.
[75] P. Mitacek, J.G. Aston, J. Am. Chem. Soc. 85 (1963) 137.
[76] G.M. Nace, J.G. Aston, J. Am. Chem. Soc. 79 (1957) 3619.
[77] G.M. Nace, J.G. Aston, J. Am. Chem. Soc. 79 (1957) 3623.
[78] G.M. Nace, J.G. Aston, J. Am. Chem. Soc. 79 (1957) 3627.
[79] E. Storms, C. Talcott-Storms, Fusion Technol. 20 (1991) 246.
[80] W. Krause, L. Kahlenberg, Trans. Electrochem. Soc. 68 (1935) 449.
[81] F.M. Mazzolai, P.G. Bordoni, F.A. Lewis, J. Phys. F 10 (1980) 781.
[82] F.M. Mazzolai, P.G. Bordoni, F.A. Lewis, J. Less-Comm. Met. 74 (1980) 137.
[83] T.B. Flanagan, J.F. Lynch, J.D. Clewley, B. Von Turkovich, J. Less-Comm. Met. 49 (1976) 13.
[84] J.F. Lynch, J.D. Clewley, T. Curran, T.B. Flanagan, J. Less-Comm. Met. 55 (1977) 153.
[85] J. Crank, The Mathematics of Diffusion (Ch. 4 and 5), Clarendon Press, Oxford, 1975.
[86] S. Majorowski, B. Baranowski, J. Phys. Chem. Solids 43 (1982) 1119.
[87] S. Majorowski, B. Baranowski, in: P. Jean, C.H. Satterthwaite (Eds.), Electronic Structure and Properties of Hydrogen in Metals, Plenum Press, New York, 1983, p. 519.
[88] W.S. Zhang, Z.L. Zhang, X.W. Zhang, F. Wu, J. Electroanal. Chem. 474 (1999) 123.
[89] M. Enyo, in: B.E. Conway, J.O.'M. Bockris, E. Yeager, S.U.M. Khan, R.E. White (Eds.), Kinetics and Mechanisms of Electrode Processes, vol. 7, Plenum Press, New York, 1983, p. 241.
[90] W.S. Zhang, X.W. Zhang, H.Q. Li, J. Electroanal. Chem. 434 (1997) 31.
[91] N. Ibl, in: E. Yeager, J.O.'M. Bockris, B.E. Conway, S. Sarangapani (Eds.), Comprehensive Treatise of Electrochemistry, vol. 6, Plenum Press, New York, 1983, p. 239.
[92] H. Vogt, in: E. Yeager, J.O.'M. Bockris, B.E. Conway, S. Sarangapani (Eds.), Comprehensive Treatise of Electrochemistry, vol. 6, Plenum Press, New York, 1983, p. 445.
[93] P.J. Sides, in: R.E. White, J.O.'M. Bockris, B.E. Conway (Eds.), Modern Aspects of Electrochemistry, vol. 18, Plenum Press, New York, 1986, p. 303.